Polarization of the prompt γ-ray emission from the γ-ray burst of 6 December 2002

Wayne Coburn* & Steven E. Boggs*†

* Space Sciences Laboratory, and † Department of Physics, University of California, Berkeley, California 94720, USA

Observations of the afterglows of γ-ray bursts (GRBs) have revealed that they lie at cosmological distances, and so correspond to the release of an enormous amount of energy[1,2]. The nature of the central engine that powers these events and the prompt γ-ray emission mechanism itself remain enigmatic because, once a relativistic fireball is created, the physics of the afterglow is insensitive to the nature of the progenitor. Here we report the discovery of linear polarization in the prompt γ-ray emission from GRB021206, which indicates that it is synchrotron emission from relativistic electrons in a strong magnetic field. The polarization is at the theoretical maximum, which requires a uniform, large-scale magnetic field over the γ-ray emission region. A large-scale magnetic field constrains possible progenitors to those either having or producing organized fields. We suggest that the large magnetic energy densities in the progenitor environment (comparable to the kinetic energy densities of the fireball), combined with the large-scale structure of the field, indicate that magnetic fields drive the GRB explosion.

We used the Reuven Ramaty High Energy Solar Spectroscopic Imager (RHESSI)[3] to make these γ-ray observations of GRB021206. RHESSI has an array of nine large-volume (300 cm^3) coaxial germanium detectors with high spectral resolution, designed to study solar X-ray and γ-ray emission (3 keV–17 MeV). RHESSI has high angular resolution (2″) in the ~1° field of view of its optics; however, the focal plane detectors are unshielded, open to the whole sky. Thus, while the chances are small that RHESSI will see a GRB in its imaging field of view, it measures them frequently in the focal plane detectors themselves. These observations provide high-resolution spectra, individual photon times and energies, as well as the potential for polarization measurements. RHESSI is not optimized to act as a γ-ray polarimeter, but several aspects of its design make it the most sensitive instrument to date for measuring astrophysical γ-ray polarization.

In the soft γ-ray range of ~0.15–2.0 MeV, the dominant photon interaction in the RHESSI detectors is Compton scattering. A small fraction of incident photons will undergo a single scatter in one detector before being scattered and/or photoabsorbed in a second separate detector, which are the events sensitive to the incident γ-ray polarization. Linearly polarized γ-rays preferentially scatter in directions perpendicular to their polarization vector. In RHESSI, this scattering property can be used to measure the intrinsic polarization of astrophysical sources. The sensitivity of an instrument to polarization is determined by its effective area to scatter events, and the average value of the polarimetric modulation factor[4,5], $\mu(\theta, E_\gamma)$, which is the maximum variation in azimuthal scattering probability for polarized photons. This factor is given by $\mu = (d\sigma_\perp - d\sigma_\parallel)/(d\sigma_\perp + d\sigma_\parallel)$, where $d\sigma_\perp$, $d\sigma_\parallel$ are the Klein–Nishina differential cross-sections for Compton scattering perpendicular and parallel to the polarization direction, respectively, which is a function of the incident photon energy E_γ, and the Compton scatter angle θ between the incident photon direction and the scattered photon direction. For a source of count rate S and fractional polarization Π_s, the expected azimuthal scatter angle distribution is $dS/d\phi = (S/2\pi)[1 - \mu_m\Pi_s\cos(2(\phi - \eta))]$, where ϕ

is the azimuthal scatter angle, η is the direction of the polarization vector, and μ_m is the average value of the polarimetric modulation factor for the instrument. Although RHESSI has a small effective area (~20 cm^2) for events that scatter between detectors, it has a relatively large modulation factor in the 0.15–2.0 MeV range, $\mu_m \approx 0.2$, as determined by Monte Carlo simulations described below.

In comparison with other γ-ray instruments (COMPTEL, BATSE) that have attempted to measure polarization in the past[5,6], RHESSI has the major advantage of quickly rotating around its focal axis (centred on the Sun) with a 4-s period. Rotation averages out the effects of asymmetries in the detectors and passive materials that could be mistaken for a modulation. Because polarimetric modulations repeat every 180°, any source lasting more than half a rotation (2 s) will be relatively insensitive to the systematic uncertainties that typically plague polarization measurements. Finally, although the RHESSI detectors have no positioning information themselves, they are relatively loosely grouped on the spacecraft, allowing the azimuthal angle for a given scatter to be determined to within $\Delta\phi = 13°$ r.m.s. This angular uncertainty will decrease potential modulations by a factor of 0.95, which is included in our calculated modulation factor.

Prompt γ-ray emission from GRB021206 was detected with RHESSI on 6 December 2002 at 22:49 UT (Fig. 1). This GRB was also observed[7] with the Interplanetary Network (IPN), which reported a 25–100 keV fluence of 1.6×10^{-4} erg cm^{-2}, and a peak flux of 2.9×10^{-5} erg cm^{-2} s^{-1}, making this an extremely bright GRB. The IPN localized[8] GRB021206 to a 57 square-arcminute
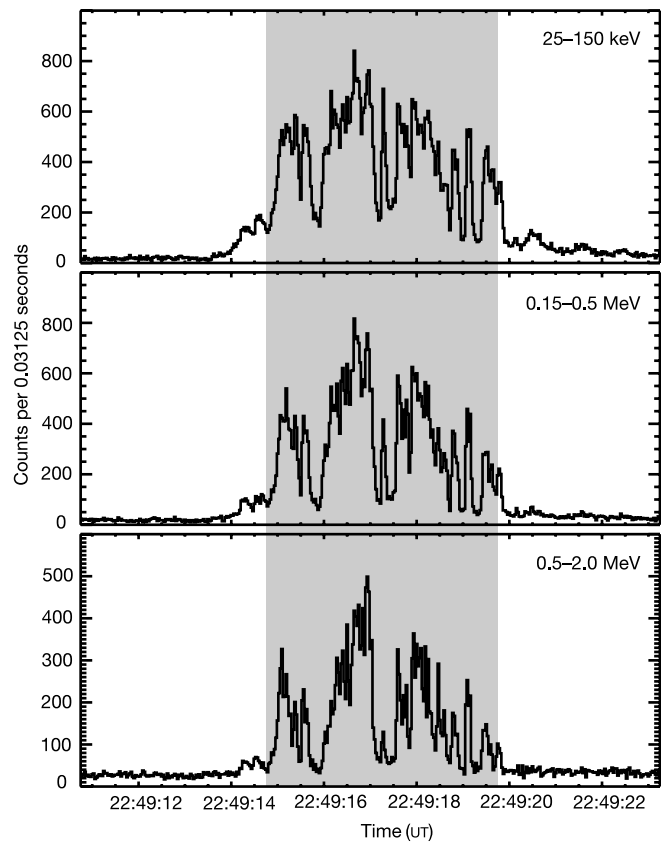

Figure 1 RHESSI light curves (in total measured counts) in three energy bins for GRB21206. The IPN localized[8] this GRB to 18° off solar, which precluded optical afterglow searches; however, the brightness, duration, and proximity to the RHESSI rotation axis made it an ideal candidate to search for polarization. The shaded region shows our 5-s integration time for the polarization analysis.

415

error box located 18° from the Sun. For RHESSI, we analysed photons in the energy range 0.15–2.0 MeV that scattered between two, and only two, detectors for the 5-s integration period shown in Fig. 1. Scattered photons constitute roughly 10% of the total 0.15–2.0 MeV light-curve events. Counts were binned by the centre-to-centre azimuthal angle between the two detectors around the RHESSI roll axis, corrected for the rotation of the spacecraft at the time of the photon event. This azimuthal distribution is plotted in Fig. 2. The top panel shows the raw data, as well as the expected variation for an unpolarized GRB due only to the light-curve variability. The bottom panel shows the residual of the data once this unpolarized distribution is subtracted. The residual shows a large modulation, which we interpret as a linear polarization of $\Pi_m = 80 \pm 20\%$. This observation is the first astrophysical polarization measurement at γ-ray energies. Note that the uncertainty on this polarization amplitude reflects in large part our uncertainty in the modulation factor. The fact that we have measured a polarization somewhere in this range has a significance of $<10^{-8}$ (or a confidence $>5.7\sigma$).

Linear polarization is generally considered a clear indication of synchrotron emission. For electrons with an energy spectrum characterized by a power-law distribution with spectral index p, synchrotron photons are emitted with a linear polarization[9] of $\Pi = (p+1)/(p+7/3)$. For shock acceleration[10], typical values of $p = 2$–3 correspond to linear polarizations of 70–75%. For unresolved sources, polarizations from many directions generally add together to produce net polarizations that are a fraction of this maximum value. While the source is unresolved in our observation, if the source electrons are moving with a bulk Doppler factor of Γ, we are only viewing the source over a solid angle $\Omega_\gamma \approx 1/\Gamma^2$. Thus, for typical values of $\Gamma \gtrsim 300$ that have been implied from GRB afterglow observations, we are effectively resolving a source region of solid angle $\Omega_\gamma \approx 10^{-5}$ sr. Our measurement of this high polarization is consistent with synchrotron origin for the initial GRB from a region of nearly uniform magnetic field. For this emission process to be radiatively efficient as is implied by many afterglow observations[11,12], the magnetic energy densities must be close to equipartition (comparable to the kinetic energy densities of the fireball)[13,14].

This polarization from the prompt γ-ray emission is significantly higher than optical polarizations of 1–3% typically measured from
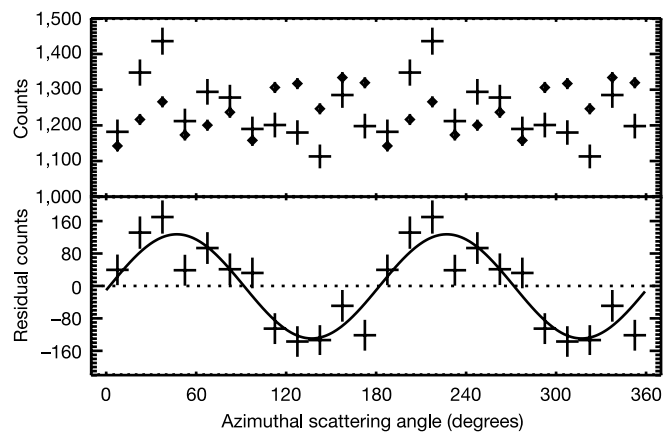
Figure 2 The azimuthal scatter distribution for the RHESSI data, corrected for spacecraft rotation. Counts were binned in 15° angular bins between 0°–180°, and plotted here twice for clarity. The top plot shows the raw measured distribution (crosses), as well as the simulated distribution for an unpolarized source (diamonds) as modelled with a Monte Carlo code, given the time-dependent incident flux. The bottom plot shows the RHESSI data with the simulated distribution subtracted. This residual is inconsistent with an unpolarized source (dashed line) at a confidence level $>5.7\sigma$. The solid line is the best-fit modulation curve, corresponding to a linear polarization of $80 \pm 20\%$.

afterglows[15–17], as well as the optical polarization of 10% recently reported[18] from the afterglow of GRB020405. The afterglow emission implies a strong magnetic field behind the shocks[19], although the field energy density can be well below equipartition[20]. However, the implied magnetic field strengths are too large to have been due to a progenitor field being dragged along by the expanding fireball[21], or compression of the ISM magnetic fields in external shocks[22]. Therefore, the magnetic fields responsible for the afterglow synchrotron emission are probably turbulent fields that have built up behind the shocks[21,23], which is consistent with the relatively small optical afterglow polarizations. This locally generated field invoked for the afterglow has influenced many researchers to consider the magnetic field responsible for the prompt burst of γ-rays as a turbulent, fireball-induced field as well. In the standard internal shock model[24], the prompt γ-rays are produced by synchrotron emission of electrons accelerated to relativistic energies by shock acceleration, requiring magnetic energy densities near equipartition in the progenitor environment. However, late-time turbulent fields have no direct implications on whether the fields responsible for the prompt γ-ray emission are predominantly turbulent or organized[21,25]. Our observation conclusively shows that the engine driving the GRB has a strong, large-scale magnetic field.

Another potential source of polarization would be as follows: if unpolarized γ-rays are initially beamed into a small-angle jet, and then scatter at an angle θ into our line of sight. The polarization induced by this Compton scattering[9] is $\Pi = (1 - \cos^2\theta)/(1 + \cos^2\theta)$ for photon energies below ~ 0.1 MeV, decreasing as the photon energy approaches and exceeds the electron rest mass, 0.511 MeV. For our energy band, we estimate a maximum Compton-induced polarization of 70% for scatter angles near 90°. However, this process would be inefficient, requiring a much larger γ-ray energy budget than the synchrotron case. First, the distribution of scattered γ-rays would be nearly isotropic, requiring an energy budget $4\pi/\Omega_j$ larger than if the observed γ-rays originated from a collimated jet of opening solid angle Ω_j. Second, to maintain such a high polarization as we observed, the γ-rays must undergo only a single scatter into our direction because secondary scatters will erase the induced polarization from the initial scatter. This condition requires that the scatter medium be optically thin, $\tau \ll 1$, and that the luminosity of the unseen initial γ-ray beam be larger than the observed scattered γ-ray emission by a factor $\sim 1/\tau$. Because Compton-scattering-induced polarization requires a total γ-ray luminosity several orders of magnitude larger than that implied by synchrotron emission, and elaborate source geometries, the synchrotron origin for the polarization is preferred.

We suggest that our observation is evidence that the magnetic fields are actually powering the GRB explosion itself. It has been argued that a 'passive' magnetic field—that is, a field dragged from the surface of central object with a magnetic dipole moment, but not driving the GRB—could not be strong enough to produce the prompt γ-ray emission without an additional locally generated turbulent magnetic field[25]. If this conclusion holds, our observation is consistent with models of a magnetically driven GRB fireball, where the driving magnetic field was generated by extracting the rotational energy of an accretion disk around a central compact object through differential rotation[26,27], by directly extracting the spin energy of a black hole threaded by magnetic field lines[28], or by extracting the spin energy of a highly magnetized neutron star[29]. Alternatively, our observation of a large-scale magnetic field could support models of dynamos in the post-shock flows[30] if the shocks can be shown to be unstable on large size scales and on timescales comparable to the prompt γ-ray emission. □

Methods

The top panel of Fig. 2 shows the azimuthal scatter distribution of 0.15–2.0 MeV events for the 5-s integration period shown in Fig. 1, corrected for the rotation of the spacecraft at the time of each photon event. This distribution is the sum of three components: the GRB

scatter event rate which averages 820 ± 8 counts per bin, the chance coincidence rate which averages 374 ± 6 counts per bin, and the background scatter event rate of 49 ± 2 counts per bin. These rates were determined and confirmed using event rates before and after the burst, combined with studies of the readout times of multiple detectors during scattered events, and were verified independently using our Monte Carlo simulations. Although the rotation will average out systematic variations in the scatter angle distribution, we still have to correct for the complex time profile of the burst itself, which will cause variations for an unpolarized source owing to the finite number of potential scatter angles RHESSI can measure at any given instant. We modelled this effect by using the 0.15–2.0 MeV total count rate in the RHESSI instrument (Fig. 1) as the time-dependent flux template for a photon transport Monte Carlo simulation, and using the time-averaged GRB photon spectrum as measured by RHESSI for our input spectrum. This simulation used the detailed RHESSI mass model that has been developed under CERN's GEANT package, allowing us to model the instrument response to a GRB at the IPN[8] sky coordinates for each rotation angle and instantaneous flux, assuming an unpolarized source. This distribution is also presented in the top panel of Fig. 2. We are looking for a modulation signal relative to this variation induced by the GRB time profile.

In the bottom panel of Fig. 2 we show the residual of the measured distribution once we have subtracted away the simulated response for an unpolarized GRB, showing our absolute modulation signal. For an unpolarized source we would expect this distribution to be flat, which we can rule out at an extremely high confidence level ($\chi^2 = 83.5$, 11 degrees of freedom, d.f.). When we fit this with a modulation curve, the fit improves significantly ($\chi^2 = 16.9$, 9 d.f.), with an amplitude of 128 ± 16 counts per bin. Statistically, this is a reasonable fit to the data (the probability of $\chi^2 > 16.9$ is 5%), but could be improved with even more detailed Monte Carlo simulations including time-dependent spectral variability. Using the count rates given above and the simulated distribution for an unpolarized GRB, we performed further numerical simulations to determine the probability that an unpolarized GRB could produce a modulation as large as the one we measure due to random Poisson counting statistics. We found this probability to be very low, $<10^{-8}$, which translates to a confidence that we have measured a polarization at a level $>5.7\sigma$. Finally, we estimated the modulation factor to be $\mu_m = 0.19 \pm 0.04$, using both a separate photon transport code which fully treats polarization in scattering and uses a simplified mass model, as well as analytical estimates based on the GEANT simulation with the full RHESSI mass model. Combining the modulation amplitude, the total source scatter event rate, and the RHESSI modulation factor, we derive a measured polarization $\Pi_m = 80 \pm 20\%$.

A number of tests were performed to check that the measured modulation is real. First, we verified that the simulated variation induced by the GRB light curve is accurate by comparing it to an angular distribution of events that were chance coincidences in two detectors. These interactions are nearly simultaneous, but separated by enough time to distinguish them as chance coincidences, not real scattered photons. This distribution should exhibit the same variations owing to the GRB light curve, but no polarization. When we subtracted the simulated distribution from the chance-coincident distribution, we found no evidence for a residual modulation. We have performed a number of independent checks to make sure we do not see modulations from other sources as well. We have verified that extended RHESSI background observations show no sign of modulations. In addition, we have done a preliminary analysis of a strong solar γ-ray flare observed on 23 July 2002, where we see some evidence for a modulation, but corresponding to a polarization $<10\%$. Therefore we feel confident that we have characterized the systematic effects in RHESSI to below the 10% polarization level.

1. Mészáros, P. Theories of gamma-ray bursts. *Annu. Rev. Astron. Astrophys.* **40,** 137–169 (2002).
2. van Paradijs, J., Kouveliotou, C. & Wijers, R. A. M. J. Gamma-ray burst afterglows. *Annu. Rev. Astron. Astrophys.* **38,** 379–425 (2000).
3. Lin, R. P. *et al.* The Reuven Ramaty High Energy Solar Spectroscopic Imager (RHESSI) mission. *Sol. Phys.* (in the press).
4. Novick, R. Stellar and solar X-ray polarimetry. *Space Sci. Rev.* **18,** 389–408 (1975).
5. Lei, F., Dean, A. J. & Hills, A. G. Compton polarimetry in gamma-ray astronomy. *Space Sci. Rev.* **82,** 309–388 (1997).
6. McConnell, M. *et al.* in *Gamma Ray Bursts, 3rd Huntsville Symposium* (eds Kouveliotou, C., Briggs, M. F. & Fishman, G. J.) *AIP Conf. Proc.* **384,** 851–855 (1996).
7. Hurley, K. *et al.* GCN Circ. 1727 (2002).
8. Hurley, K. *et al.* GCN Circ. 1728 (2002).
9. Rybicki, G. B. & Lightman, A. P. *Radiative Processes in Astrophysics* 180–181 (JWS, New York, 1979).
10. Blandford, R. & Eichler, D. Particle acceleration at astrophysical shocks—a theory of cosmic-ray origin. *Phys. Rep.* **154,** 1–75 (1987).
11. Frail, D. A., Waxman, E. & Kulkarni, S. R. A 450 day light curve of the radio afterglow of GRB 970508: fireball calorimetry. *Astrophys. J.* **537,** 191–204 (2000).
12. Freedman, D. & Waxman, E. On the energy of gamma-ray bursts. *Astrophys. J.* **547,** 922–928 (2001).
13. Derishev, E. V., Kocharovsky, V. V. & Kocharovsky, Vl. V. Physical parameters and emission mechanism in gamma-ray bursts. *Astron. Astrophys.* **372,** 1071–1077 (2001).
14. Guetta, D., Spada, M. & Waxman, E. Efficiency and spectrum of internal gamma-ray burst shocks. *Astrophys. J.* **557,** 399–407 (2001).
15. Covino, S. *et al.* GRB 990510: linearly polarized radiation from a fireball. *Astron. Astrophys.* **348,** L1–L4 (1999).
16. Wijers, R. A. M. J. *et al.* Detection of polarization in the afterglow of GRB 990510 with the ESO Very Large Telescope. *Astrophys. J.* **523,** L33–L36 (1999).
17. Rol, E. *et al.* GRB 990712: first indication of polarization variability in a gamma-ray burst afterglow. *Astrophys. J.* **544,** 707–711 (2000).
18. Bersier, D. *et al.* The strongly polarized afterglow of GRB 020405. *Astrophys. J.* **583,** L63–L66 (2003).
19. Waxman, E. γ-ray burst afterglow: confirming the cosmological fireball model. *Astrophys. J.* **489,** L33–L36 (1997).
20. Galama, T. J. *et al.* The effect of magnetic fields on γ–ray bursts inferred from multi-wavelength observations of the burst of 23 January 1999. *Nature* **398,** 394–399 (1999).
21. Medvedev, M. K. & Loab, A. Generation of magnetic fields in the relativistic shock of gamma-ray burst sources. *Astrophys. J.* **526,** 697–706 (1999).
22. Sari, R., Narayan, R. & Piran, T. Cooling timescales and temporal structure of gamma-ray bursts. *Astrophys. J.* **473,** 204–218 (1996).
23. Gruzinov, A. & Waxman, E. Gamma-ray burst afterglow: polarization and analytic light curves. *Astrophys. J.* **511,** 852–861 (1999).
24. Rees, M. J. & Mészáros, P. Unsteady outflow models for cosmological gamma-ray bursts. *Astrophys. J.* **430,** L93–L96 (1994).
25. Spruit, H. C., Daigne, F. & Drenkhahn, G. Large scale magnetic fields and their dissipation in GRB fireballs. *Astron. Astrophys.* **369,** 694–705 (2001).
26. Thompson, C. A model of gamma-ray bursts. *Mon. Not. R. Astron. Soc.* **270,** 480–498 (1994).
27. Mészáros, P. & Rees, M. J. Poynting jets from black holes and cosmological gamma-ray bursts. *Astrophys. J.* **482,** L29–L32 (1997).
28. Blandford, R. D. & Znajek, R. L. Electromagnetic extraction of energy from Kerr black holes. *Mon. Not. R. Astron. Soc.* **179,** 433–456 (1977).
29. Usov, V. V. Millisecond pulsars with extremely strong magnetic fields as a cosmological source of gamma-ray bursts. *Nature* **357,** 472–474 (1992).
30. Gruzinov, A. Gamma-ray burst phenomenology, shock dynamo, and the first magnetic fields. *Astrophys. J.* **563,** L15–L18 (2001).

Experimental entanglement purification of arbitrary unknown states

Jian-Wei Pan, Sara Gasparoni, Rupert Ursin, Gregor Weihs & Anton Zeilinger

Institut für Experimentalphysik, Universität Wien, Boltzmanngasse 5, 1090 Wien, Austria

Distribution of entangled states between distant locations is essential for quantum communication[1–3] over large distances. But owing to unavoidable decoherence in the quantum communication channel, the quality of entangled states generally decreases exponentially with the channel length. Entanglement purification[4,5]—a way to extract a subset of states of high entanglement and high purity from a large set of less entangled states—is thus needed to overcome decoherence. Besides its important application in quantum communication, entanglement purification also plays a crucial role in error correction for quantum computation, because it can significantly increase the quality of logic operations between different qubits[6]. Here we demonstrate entanglement purification for general mixed states of polarization-entangled photons using only linear optics[7]. Typically, one photon pair of fidelity 92% could be obtained from two pairs, each of fidelity 75%. In our experiments, decoherence is overcome to the extent that the technique would achieve tolerable error rates for quantum repeaters in long-distance quantum communication[8]. Our results also imply that the requirement of high-accuracy logic operations in fault-tolerant quantum computation can be considerably relaxed[6].

The resource of quantum entanglement has many important applications in quantum information processing (QIP). In quantum communication, the generation of entanglement between distant